Neurol Sci (2014) 35:753–758
DOI 10.1007/s10072-013-1595-2

ORIGINAL ARTICLE

Substantia nigra in Parkinson's disease: a multimodal MRI comparison between early and advanced stages of the disease

Domenico Aquino · Valeria Contarino · Alberto Albanese · Ludovico Minati · Laura Farina · Marina Grisoli · Antonio Elia · Maria Grazia Bruzzone · Luisa Chiapparini

Received: 3 July 2013 / Accepted: 28 November 2013 / Published online: 11 December 2013
© Springer-Verlag Italia 2013

Abstract This study focused on the substantia nigra (SN) in Parkinson's disease (PD). We measured its area and volume, mean diffusivity (MD), fractional anisotropy (FA) and iron concentration in early and late PD and correlated the values with clinical scores. Twenty-two early PD (EPD), 20 late PD (LPD) and 20 healthy subjects (age 64.7 ± 4.9, 60.5 ± 6.1, and 61 ± 7.2 years, respectively) underwent 1.5 T MR imaging with double-TI-IR T1-weighted, T2*-weighted and diffusion tensor imaging scans. Relative SN area, MD, FA and R2* were measured in ROIs traced on SN. Correlation with Unified Parkinson Disease Rating Scale (UPDRS) scores was assessed. In LPD, the SN area was significantly reduced with respect to EPD ($p = 0.04$) and control subjects ($p < 0.001$). In EPD, the SN area was also significantly smaller than in controls ($p = 0.006$). Similarly, the SN volume significantly differed between LPD and controls ($p = 0.001$) and between EPD and LPD ($p = 0.049$), while no significant differences were found between controls and EPD. Both SN area ($r = 0.47$, $p = 0.004$) and volume ($r = 0.46$, $p = 0.005$) correlated with UPDRS scores. At 1.5 T, SN morphological measurements were sensitive to early PD changes and able to track the disease progression, while MD and FA measures and relaxometry did not provide significant results.

Keywords Parkinson disease · UPDRS · Substantia nigra · Inversion recovery · Diffusion tensor imaging · Relaxometry

D. Aquino (✉) · V. Contarino · L. Farina · M. Grisoli · M. G. Bruzzone · L. Chiapparini
Neuroradiology Department, IRCCS Foundation Neurological Institute Carlo Besta, Via Celoria, 11, 20133 Milan, Italy
e-mail: aquino@istituto-besta.it

A. Albanese · A. Elia
1st Neurology Unit, IRCCS Foundation Neurological Institute Carlo Besta, Milan, Italy

L. Minati
Scientific Department, IRCCS Foundation Neurological Institute Carlo Besta, Milan, Italy

Introduction

Parkinson's disease (PD) is a neurodegenerative disorder clinically characterized by bradykinesia, rigidity and tremor at rest. The disease usually begins on one side and follows a progressive course becoming bilateral over the years. The major pathological hallmark is a massive selective loss of pigmented neurons in the substantia nigra (SN) associated with the presence of Lewy bodies and neurites in specific regions of the brain [1]. At least 70–80 % of dopaminergic neurons in the pars compacta of the SN (SNc) are lost before the onset of the clinical symptoms of PD.

Currently, diagnosis of PD still relies on clinical assessment, both in early and advanced stages [2, 3]. Conventional MRI is of scarce utility for the diagnosis of PD, whereas it can be valuable in investigating atypical parkinsonian disorders [4]. Radiolabeled tracer imaging techniques such as PET and SPECT that may reveal striatal neuronal loss by showing a reduction in striatal dopaminergic nerve terminals [5–7] may be considered as the gold standard because of their high sensitivity and ability to distinguish between PD and other parkinsonian disorders. These techniques are also useful to monitor the evolution of the disease and the efficacy of available treatments [8]. However, these examinations are invasive and expensive, therefore, not commonly used for routine diagnosis and follow-up of PD.

Advanced MRI methods, on the other hand, may identify subtle changes in the SN, that may be important for the diagnosis of preclinical and early stage of PD, for monitoring the progression of the disease and the efficacy of treatments. Hutchinson and Raff [9] and Minati et al. [10] independently, showed a significant difference between controls and PD patients in the SN area measured on particular combinations of inversion recovery (IR)-weighted images. Analysis of diffusion tensor imaging (DTI) in PD patients demonstrated changes in fractional anisotropy (FA) values in the SN, suggesting micro-structural modifications [11]. Since iron deposition in the SN is thought to be related to the pathogenesis of PD [12–14], iron content was evaluated with MR relaxometry in high-field strength units [12, 15] with demonstration of increased early deposition.

Since a single advanced MRI technique, however, might be insufficient to effectively detect early PD patients, integration of different unconventional methods at high-field MR (3.0 T) was proposed for the identification of the pathological changes and to monitor the progression of the disease [16, 17].

The most widely used clinical field strength remains 1.5 T, but, to date, a multimodal MR study of PD focusing on the involvement of the SN in both early and advanced stages of the disease at this field strength has not been carried out.

The aim of this study was to evaluate on a 1.5 T unit if the extent of SN shrinkage, microstructural changes revealed by mean diffusivity (MD) and FA modifications, and the iron accumulation differ between PD patients in the early (EPD) and in the late stages of the disease (LPD), in comparison with controls and to correlate these measurements with the clinical severity of motor symptoms.

Materials and methods

Participants

The study complied with institutional guidelines and regulations. All subjects gave written, informed consent for research use of scanning in accordance with the Declaration of Helsinki.

Patients

Forty-two patients were enrolled, 22 in EPD group and 20 in LPD group; the demographic and main clinical features are summarized in Table 1. The patients, who had not been included in previous studies, were enrolled consecutively and met the following inclusion criteria: (1) diagnosis of idiopathic PD according to the British PD Society Brain Bank criteria [18]; (2) disease duration between 3 and 5 years (EPD group), or between 6 and 10 years (LPD group); (3) age between 50 and 75 years; (4) taking dopaminergic medication and with successful control of motor symptoms; (5) Hoehn and Yahr [19] stage III or less, on-treatment; (6) Milan overall dementia assessment [20] score 90/100 or more. Patients were excluded if they presented severe rest tremor preventing MRI scanning, if they had motor complications (wearing off and dyskinesias), and if they were under treatment with deep brain stimulation, jejunal levodopa, or subcutaneous apomorphine. The levodopa equivalent daily dose (LEDD, measured in milligrams) was calculated by adding to the standard levodopa dose all dopaminergic medications converted to relative potency of standard levodopa [21]. Motor symptoms were assessed using the Unified Parkinson's Disease Rating Scale (UPDRS-III) [22].

Table 1 Demographic features and clinical state of the patients (mean ± SD)

	EPD group	LPD group
Age at onset	60.7 ± 4.9*	52.5 ± 6.4
Age at time of evaluation (years)	64.7 ± 4.9**	60.5 ± 6.1
Disease duration (years)	4.0 ± 0.8*	7.9 ± 1.6
Gender (% female)	54	40
Oral therapy (LEDD)	393.4 ± 221.7*	788.8 ± 358.6
UPDRS-III under therapy	18.0 ± 7.1	22.9 ± 10.9

* Significantly different ($p < 0.01$) from advanced Parkinson's disease; ** significantly different ($p < 0.05$) from advanced Parkinson's disease

Healthy controls

Twenty control subjects (CS) (61 ± 7.26 years, 50 % female) were recruited, mainly from the hospital staff. Controls were examined to exclude clinical and neuroradiological evidence of neurological diseases.

Neuroimaging

MRI acquisition

Scans were performed on a Magnetom Avanto 1.5 T Scanner (Siemens, Erlangen, Germany). The MRI acquisition protocol was the following: (1) volumetric sagittal T1 magnetization-prepared rapid gradient-echo (MPRAGE) (TR = 1,640 ms, TI = 552 ms, TE = 2.48 ms, FOV = 256 × 256 mm, matrix = 256 × 256, slice thickness = 1 mm, intersection gap 0 mm) sequence; (2) axial double-echo proton-density and T2-weighted (TR = 3,500 ms, TE = 17 and 84 ms, FOV = 230 × 187 mm, matrix = 256 × 208, slice thickness = 6 mm, intersection gap = 10 %) sequences; (3) axial IR (TR = 3,000 ms, TI = 470/240 ms, TE = 12 ms, FOV = 160 × 120 mm, matrix =

96 × 128, slice thickness = 1.5 mm, intersection gap = 0 mm) sequences. The parameters of these two sequences, white matter-suppressed (WMS) and gray matter-suppressed (GMS), respectively, were adjusted to minimize signal intensity of the white matter and gray matter; (4) DTI spin-echo (TR = 9,200 ms, TE = 100 ms, FOV = 281 × 281 mm, matrix = 128 × 128, slice thickness = 2.2 mm, intersection gap = 0, 64 collinear directions with 8 $b = 0$ and maximum b value = 1,200 s/mm^2); (5) GRE-multiecho sequence to evaluate iron deposition (TR = 1,140 ms, TE = 5/55 ms in 12 echo times with 5 ms interval, FOV = 280 × 210 mm, matrix = 192 × 256, slice thickness = 5 mm, intersection gap 1 mm).

Image processing

SN area and volume estimate

The two inversion times of the IR sequence were chosen to highlight the gray matter/white matter contrast and, consequently, the extent of the intact SN [23]. The TI = 240 ms sequence was subtracted from the TI = 470 ms sequence to obtain a final sequence in which the contrast appears maximized.

SN MD and FA measures

First, eddy current distortions were corrected on the DTI by means of the FMRIB Linear Image Registration Tool (FMRIB, University of Oxford, Oxford, UK, http://www.fmrib.ox.ac.uk/fsl/). Then, each non-diffusion weighted volume was co-registered with the first one and the co-registration parameters were applied to the 64 directions. The diffusional parameters (MD, FA and colormaps) were thereafter computed with Basser's method [24].

Iron concentration estimate

R2* (=1/T2*) maps were calculated in each subject. The signal intensity decay was expressed with a monoexponential model using the following expression:

$$S(t) = S(0) \cdot e^{-\frac{TE}{T2*}} + C$$

where $S(t)$ is the signal intensity at time t, $S(0)$ the initial signal intensity and C is the offset signal of the system [25, 26].

ROI positioning and measures

SN area and volume

ROIs were drawn by two senior neuroradiologists blinded to the clinical data on axial IR sections to delineate the SN and mesencephalon. Given the anatomic variability between subjects, mesencephalon area was measured to normalize the SN area (relative area). As discussed previously [10], the mesencephalon is a preferable reference here, as it is the gross anatomical structure most clearly related to the SN; correcting on the basis of whole brain measurements such as total intracranial volume would have left in substantial variability related to the varying proportion of mesencephalon size with respect to whole brain size. Importantly, normalization with respect to the mesencephalon also has the consequence of removing the effect on unspecific atrophy, which was not of interest here as the focus was limited to the SN. The SN, visible as a hypointense area including both the pars compacta and the pars reticulata, was delineated by drawing the profile of this structure in each section. The area measurement was calculated separately for each side [27] and the average was considered.

For each subject, approximate volumes were determined as the sum of the absolute SN areas multiplied by the slice thickness (1.5 mm) and number of slices.

SN mean diffusivity and fractional anisotropy

The same neuroradiologists drew polygonal ROIs on the FA colormaps on both SN; these maps were chosen as they provide better anatomical contrast with surrounding structures than FA or MD alone. The ROIs were then overlapped to MD and FA maps to estimate the corresponding mean values. All ROI drawing and measurement were performed using ImageJ (National Institutes of Health, Bethesda, MD, http://rsbweb.nih.gov/ij/).

Iron concentration

A planar ROI was drawn on the SN on the sixth echo-time of the GRE sequence (Fig. 1). This echo-time was chosen as the best trade-off between anatomical contrast and distortion due to susceptibility inhomogeneity.

Statistical analysis

Prior to statistical analysis, the effect of age was removed by linear regression. A one-way analysis of variance (ANOVA) was used to evaluate group differences between CS, EPD and LPD groups, for SN relative area and volume, MD, FA and R2* measured in the SN followed by post hoc t tests. A Kruskal–Wallis test was performed to exclude differences in the number of SN slices, evaluated by the two examiners. Differences between the three groups were assessed using Bonferroni corrected non-paired t tests.

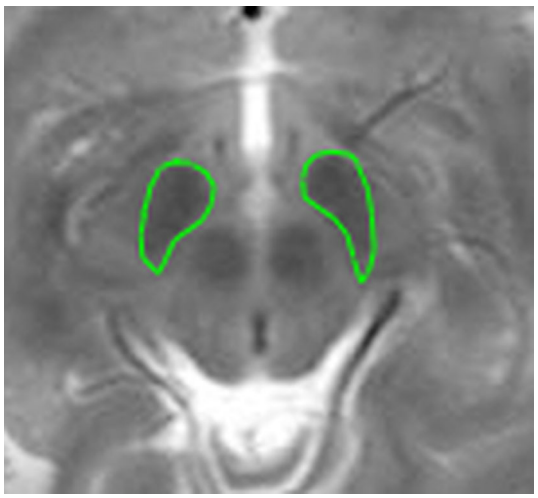

Fig. 1 Axial T2-weighted image demonstrating the regions of interest (ROIs) used to measure SN area and volume for an arbitrarily chosen subject. The ROIs were placed symmetrically on the *left* and *right portion* of the SN in all the sections where the edges of the structure resulted clearly distinguishable

Results

Relative SN area and volume estimate

A significant correlation between the measurements made by the two neuroradiologists was found ($p < 0.05$). Relative SN area and volume of each group (EPD, LPD and controls) are plotted in Fig. 2.

The ANOVA on relative SN area measured on IR images and averaged between the two sets evaluated by the two examiners indicated that the relative SN area decreased from CS to early PD stage and further from EPD stage to LPD stage (CS 0.13 ± 0.16; EPD 0.11 ± 0.16; LPD 0.10 ± 0.01). There were significant differences among groups ($F(2,52) = 16.9$, $p < 0.001$). The post hoc test provided significant p value for LPD group versus CS group ($p < 0.001$, mean difference 0.030 ± 0.005), EPD group versus CS group ($p = 0.04$, mean difference 0.017 ± 0.005) and LPD group versus EPD group ($p = 0.01$, mean difference 0.013 ± 0.005).

The averaged relative volumes of SN were 0.44 ± 0.120, 0.39 ± 0.10 and 0.31 ± 0.96 for CS group, EPD group and LPD group, respectively. The ANOVA indicated significant differences among groups ($F(2,52) = 7.5$, $p = 0.001$). The post hoc tests showed significant differences between LPD group and CS group ($p = 0.001$) and between LPD group and EPD group ($p = 0.049$), while no significant differences were found between CS and EPD patients. Using a Kruskal–Wallis test on the number of SN slices, no significant difference was found among the three groups.

A Pearson's coefficient of $r = 0.47$ ($p = 0.004$) was found in the correlation analysis between SN area and

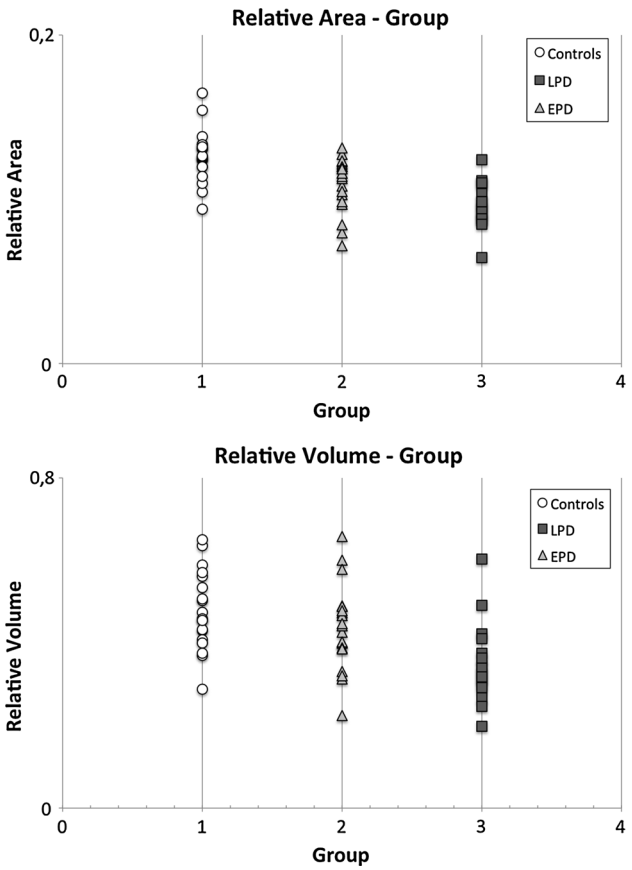

Fig. 2 Plot of the SN relative area and volume values in each group: SN extension reduces progressively with disease severity

UPDRS scores. The correlation coefficient between SN volumes and UPDRS in LPD versus EPD was significant $r = 0.46$ ($p = 0.005$) (Fig. 3).

SN MD and FA measure

The ANOVA demonstrated no significant differences among groups in the MD and FA values. A significant correlation between the two sets was observed ($p < 0.01$). The regression analysis on MD and UPDRS scores values was not significant.

Iron concentration estimate

The ANOVA showed no significant differences among groups in the R2* values. A significant correlation between the two sets was found ($p < 0.01$). The regression analysis on R2* values and UPDRS scores was not significant.

Discussion

We compared PD patients with different disease duration, EPD and LPD, versus controls. The extension of the SN, its

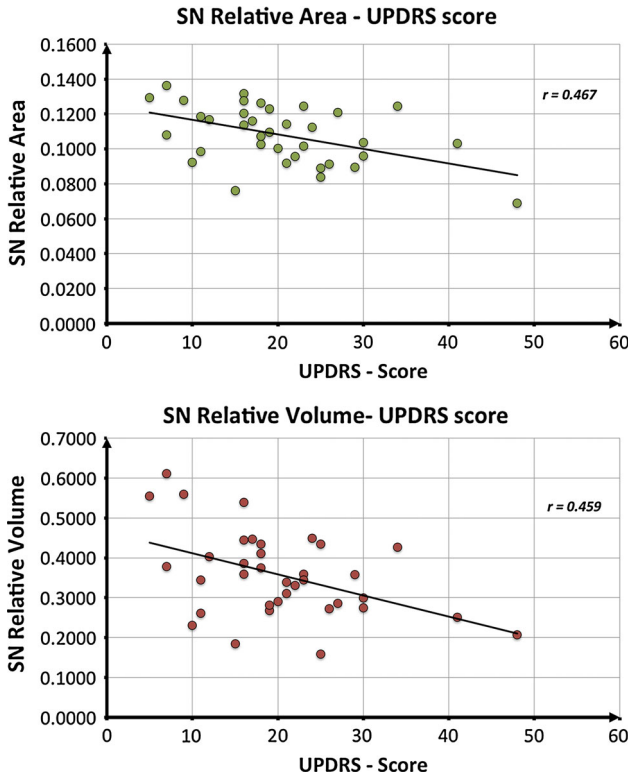

Fig. 3 Correlation between UPDRS scores and: SN relative area ($r = 0.47$); SN relative volume ($r = 0.46$)

MD and FA and iron concentration have all previously been demonstrated to correlate with disease severity and progression [15]. Combination of multiple measurements might provide greater diagnostic power in comparison to single measurements. However, the only significant differences we obtained were for SN area and volume. In line with previous studies [10, 23], we demonstrated a decrease in the total SN area with increasing clinical severity. The differences in the SN area are significant in the comparison between LPD and EPD, in the comparison between EPD and controls, and in the comparison between LPD and controls. Progressive shrinkage and alteration of the SN due to neuronal loss and gliosis may be used as a diagnostic tool to monitor disease severity and progression. The linear regression between the SN area and volume and the UPDRS scores also showed a good correlation with the progression of the disease (Fig. 3).

Differently from measurements of the SN relative area, measurements of the SN relative volumes provided similar results in the comparison between LPD and CS and between LPD and EPD, but did not find differences between CS and EPD, suggesting insufficient sensitivity of this technique in detecting the subtle changes of the early stages of the disease. This, however, is in contradiction to the known pathological changes of PD: early clinical parkinsonian signs appear when the cell loss in the SN reaches 70–80 % of the normal population [24]. We hypothesize that bulk loss of neuronal cells may not represent the main element that determines the global SN alteration as seen by IR imaging, but it is also possible that this method of approximating volume was not sufficiently accurate.

Notably, measurements of MD and FA showed no significant differences between groups. Based on previous work, we expected increased MD [27] and decrease FA on the basis of neuronal loss and tissue damage. Three possible explanations may be proposed: (1) the reduction of the number of neurons in the SN could not be sufficient to determine detectable tissue abnormalities; (2) the gliosis and the presence of Lewy bodies, known to occur in PD, might mask the changes induced by neuronal loss and reduce the water-free molecules diffusivity; (3) the number of patients was insufficient.

The R2* values also showed no significant differences between groups. We ascribe this null finding result mainly to the high variability of the SN iron content in the age range under study in addition to the changes determined by the pathological condition [25, 26]. However, as other studies at 3T had found significant effects [28], it is possible that the measurement accuracy, in terms of SNR and geometric distortions, was not adequate on the scanner under consideration.

With respect to the null findings from the DTI and R2* measurements, the present investigation should be treated as preliminary. Since previous works have demonstrated significant changes [28–30], our results do not imply that EPD, LPD patients and controls are truly overlapping on these measurements. Rather, our results suggest that on a clinical 1.5 T scanner and a relatively small sample, it may be easier to find significant effects with IR measurements, rather than DTI and R2* measurements. It should also be noted that the measurements were conducted in different geometric spaces. While this is a limitation of the present study, the SN was clearly identifiable on the DTI and R2* maps, so it was preferred to perform ROI tracing separately to avoid co-registration errors due to distortion.

Another feature that might have interfered with our findings is the demographic differences between the two groups: LPD patients were younger and with earlier age at onset than EPD patients. This might be related to our strict inclusion criteria which lead us to exclude a few LPD patients who had a more severe degree of the disease which prevented the possibility of obtaining adequate neuroradiological studies. Indeed, the significant age mismatch between EPD and LPD and consequently between EPD and healthy controls should make difficult to distinguish if the reduction of SN area/volume might be due to the disease or to physiological effects of aging. While we corrected all measurements for age, the possibility of residual confounding effects remains (Fig. 2).

It must be noted that the technique applied requires an accurate volume acquisition positioning and is tracer dependent, due to the difficulty in delineating the fuzzy and irregular edges of SN [10]. Further, ROI tracing is a time-consuming task. To reduce the tracer-dependent error, optimization of sequence geometry and/or the use of more than two inversion times to obtain a better contrast, may be proposed. The new available tools that allow placing the volume of acquisition in the correct position on the basis of anatomical landmarks automatically identified will make this method easily reproducible.

In conclusion, in PD patients studied at 1.5 T advanced MR techniques are not sufficiently helpful in evaluating the SN. Therefore, they should not be recommended for this purpose. If accurate clinical evaluation of PD patients needs to be supported by MR imaging advanced techniques, they should be obtained at higher fields.

Acknowledgments This work was funded by the Italian Ministry of Health, RF 110 (ex art 56), year 2010.

Conflict of interest There were no real or perceived conflicts of interest.

References

1. Halliday G, Lees A, Stern M (2011) Milestones in Parkinson's disease—clinical and pathologic features. Mov Disord 26:1015–1021
2. Seppi K, Poewe W (2010) Brain magnetic resonance imaging techniques in the diagnosis of parkinsonian syndromes. Neuroimaging Clin N Am 20:29–55
3. Dickson DW, Braak H, Duda JE et al (2009) Neuropathological assessment of Parkinson's disease: refining the diagnostic criteria. Lancet Neurol 8:1150–1157
4. Chahine LM, Stern MB (2011) Diagnostic markers for Parkinson's disease. Curr Opin Neurol 24:309–317
5. Wilson JM, Levey AI, Rajput A et al (1996) Differential changes in neurochemical markers of striatal dopamine nerve terminals in idiopathic Parkinson's disease. Neurology 47:718–726
6. Innis RB, Seibyl JP, Scanley BE et al (1993) Single photon emission computed tomographic imaging demonstrates loss of striatal dopamine transporters in Parkinson disease. Proc Natl Acad Sci USA 90:11965–11969
7. Leenders KL, Oertel WH (2001) Parkinson's disease: clinical signs and symptoms, neural mechanisms, positron emission tomography, and therapeutic interventions. Neural Plast 8:99–110
8. Thobois S, Jahanshahi M, Pinto S, Frackowiak R, Limousin-Dowsey P (2004) PET and SPECT functional imaging studies in Parkinsonian syndromes: from the lesion to its consequences. Neuroimage 23:1–16
9. Hutchinson M, Raff U (2008) Detection of Parkinson's disease by MRI: spin–lattice distribution imaging. Mov Disord 23: 1991–1997
10. Minati L, Grisoli M, Carella F, De Simone T, Bruzzone MG, Savoiardo M (2007) Imaging degeneration of the substantia nigra in Parkinson disease with inversion-recovery MR imaging. AJNR Am J Neuroradiol 28:309–313
11. Vaillancourt DE, Spraker MB, Prodoehl J et al (2009) High-resolution diffusion tensor imaging in the substantia nigra of de novo Parkinson disease. Neurology 72:1378–1384
12. Sian-Hülsmann J, Mandel S, Youdim MB, Riederer P (2011) The relevance of iron in the pathogenesis of Parkinson's disease. J Neurochem 118(6):939–957
13. Carroll CB, Zeissler ML, Chadborn N et al (2011) Changes in iron-regulatory gene expression occur in human cell culture models of Parkinson's disease. Neurochem Int 59:73–80
14. Martin WR, Wieler M, Gee M (2008) Midbrain iron content in early Parkinson disease: a potential biomarker of disease status. Neurology 70:1411–1417
15. Péran P, Cherubini A, Assogna F et al (2010) Magnetic resonance imaging markers of Parkinson's disease nigrostriatal signature. Brain 133:3423–3433
16. Cherubini A, Péran P, Caltagirone C, Sabatini U, Spalletta G (2009) Aging of subcortical nuclei: microstructural, mineralization and atrophy modifications measured in vivo using MRI. Neuroimage 48:29–36
17. Hutchinson M, Raff U (1999) Parkinson's disease: a novel MRI method for determining structural changes in the substantia nigra. J Neurol Neurosurg Psychiatry 69:815–818
18. Hughes AJ, Daniel SE, Kilford L, Lees AJ (1992) Accuracy of clinical diagnosis of idiopathic Parkinson's disease: a clinico-pathological study of 100 cases. J Neurol Neurosurg Psychiatry 55:181–184
19. Hoehn MM, Yahr MD (1967) Parkinsonism: onset, progression and mortality. Neurology 17:427–442
20. Brazzelli M, Capitani E, Della Sala S, Spinnler H, Zuffi M (1994) A neuropsychological instrument adding to the description of patients with suspected cortical dementia: the Milan overall dementia assessment. J Neurol Neurosurg Psychiatry 57:1510–1517
21. Romito LM, Contarino MF, Vanacore N, Bentivoglio AR, Scerrati M, Albanese A (2009) Replacement of dopaminergic medication with subthalamic nucleus stimulation in Parkinson's disease: long-term observation. Mov Disord 24:557–563
22. Fahn S, Elton RL (1987) Members of the UPDRS Development Committee. Unified Parkinsons disease rating scale. In: Fahn S, Marsden CD, Calne D, Goldstein M (eds) Recent developments in Parkinsons disease, 2nd edn. Macmillan Healthcare Information, Florham Park, pp 153–163
23. Raff U, Hutchinson M, Rojas GM, Huete I (2006) Inversion recovery MRI in idiopathic Parkinson disease is a very sensitive tool to assess neurodegeneration in the substantia nigra: preliminary investigation. Acad Radiol 13:721–727
24. Basser PJ, Pierpaoli C (1996) Microstructural and physiological features of tissues elucidated by quantitative-diffusion-tensor MRI. J Magn Reson B 111:209–219
25. Hallgren B, Sourander P (1958) The effect of age on the non-haemin iron in the human brain. J Neurochem 3:41–51
26. Aquino D, Bizzi A, Grisoli M, Garavaglia B, Bruzzone MG, Nardocci N (2009) Age-related iron deposition in the basal ganglia: quantitative analysis in healthy subjects. Radiology 252:165–172
27. Gattellaro G, Minati L, Grisoli M, Mariani C, Carella F, Bruzzone MG (2009) White matter involvement in idiopathic Parkinson disease: a diffusion tensor imaging study. AJNR Am J Neuroradiol 30:1222–1226
28. Du G, Lewis MM, Styner M, Shaffer ML, Sen S, Yang QX, Huang X (2011) Combined R2* and diffusion tensor imaging changes in the substantia nigra in Parkinson's disease. Mov Disord 26:1627–1632
29. Meijer FJA, Bloem RB, Mahlknecht P, Seppi K, Goraj B (2013) Update on diffusion MRI in Parkinson's disease and atypical parkinsonism. J Neurol Sci 332(2013):21–29
30. Chan LL, Rumpel H, Yap K, Lee E, Loo HV, Ho GL et al (2007) Case control study of diffusion tensor imaging in Parkinson's disease. J Neurol Neurosurg Psychiatry 78(12):1383–1386